Hydrodynamics, heat and mass transfer during crystal growth in assembly of "Hele-Shaw" cells

Cite as: AIP Conference Proceedings **2302**, 070002 (2020); https://doi.org/10.1063/5.0033603
Published Online: 03 December 2020

A. Prostomolotov, and N. Verezub

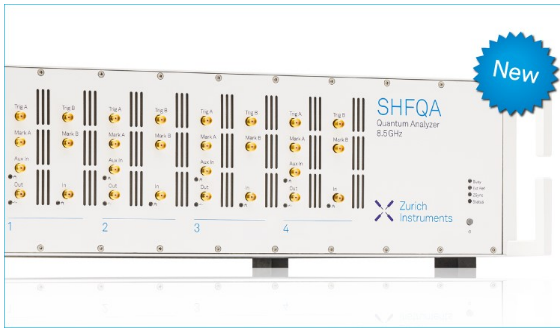

Hydrodynamics, Heat and Mass Transfer during Crystal Growth in Assembly of “Hele-Shaw” Cells

A. Prostomolotov [a] and N. Verezub [b]

Ishlinsky Institute for Problems in Mechanics RAS, 101 Vernadskii Ave., Bl. 1, 119526 Moscow, Russia

[a] Corresponding author: prosto@ipmnet.ru
[b]verezub@ipmnet.ru

Abstract. The physicochemical processes are studied in a new modification of Bridgman’s crystal growth by way of a “cassette” crystallization in the assembly of “Hele-Shaw” cells for producing the polycrystalline bismuth telluride, which is used for thermoelectric applications. The aim was associated with the study of heat and mass transfer processes for the elimination of an instability of polycrystalline growth in the form of dendritic formations. It was established an influence of a crystallization rate on a chemical and phase micro inhomogeneity arising in the polycrystalline bismuth telluride. Negative affection of a large crystallization rate on the thermoelectric and mechanical properties of grown bismuth telluride wafers is discussed.

INTRODUCTION

The fundamental tasks of microstructure formation and improving the thermoelectric (TE) properties occur for technologies of the plastic molding and melt crystallization of TE materials on the basis of solid bismuth telluride solutions.

At the present time the plastic molding methods are widely used, in which an influence of intense plastic deformations on microstructure formation and TE properties play a decisive importance. For semiconductor TE materials, as well as for metals, such intense deformations provide the formation of ultrafine-grained structures with grain sizes of 100–200nm [1].

The ECAP process is a promising way of intensive mechanical deformations. The ECAP scheme for producing TE materials based on solid solutions of chalcogenides is presented in [2].

Since of 50s previous century TE materials production by a melt crystallization were carried out by classical Bridgman's method of crystal growth. However lately the most effective method has been proposed on the basis of “cassette” modification of classical Bridgman’s method [3,4] as the assembly of “Hele-Shaw” cells for growing crystalline wafers of TE materials based on bismuth telluride solid solutions.

Thanks to the original modification, such process for growing crystalline plates has comparative simplicity and high productivity. As a result of directed crystallization, a more perfect crystalline structure of the material is formed. This structure has smaller angles of deviation of cleavage planes due to the possibilities of effecting on their orientations during crystal growth.

In this work, both the patents [3,4] and the results of technological studies carried out in National Research Technological University (MISiS) [5] were used as the basis for an elaboration of the mathematical models. As a result, Bridgman's multi cassette method was presented as the assembly of Hele-Shaw cells and the elaborated mathematical models allowed to carry out a radiation-conducting analysis of thermal processes in whole volume of hot zone and a convective analysis of heat-mass transfer in separate cassette.

Application of Mathematics in Technical and Natural Sciences
AIP Conf. Proc. 2302, 070002-1–070002-8; https://doi.org/10.1063/5.0033603
Published by AIP Publishing. 978-0-7354-4036-4/$30.00

FORMULATION OF THE PROBLEM

The scheme of mathematical model for heat and mass transfer processes in a separate cassette is shown in Fig. 1a. The cassette consists of graphite shell (I), in which there are a number of cavities. The main cavity contains crystallizing melt (II), the cavity having the crystal seed (III), the transport channels for melt filling of cassette (IV) and the holes for assembling the cassettes into blocks (V). Total sizes of single cassette ($x \times y \times z$): 4.4×6×1.3cm^3.

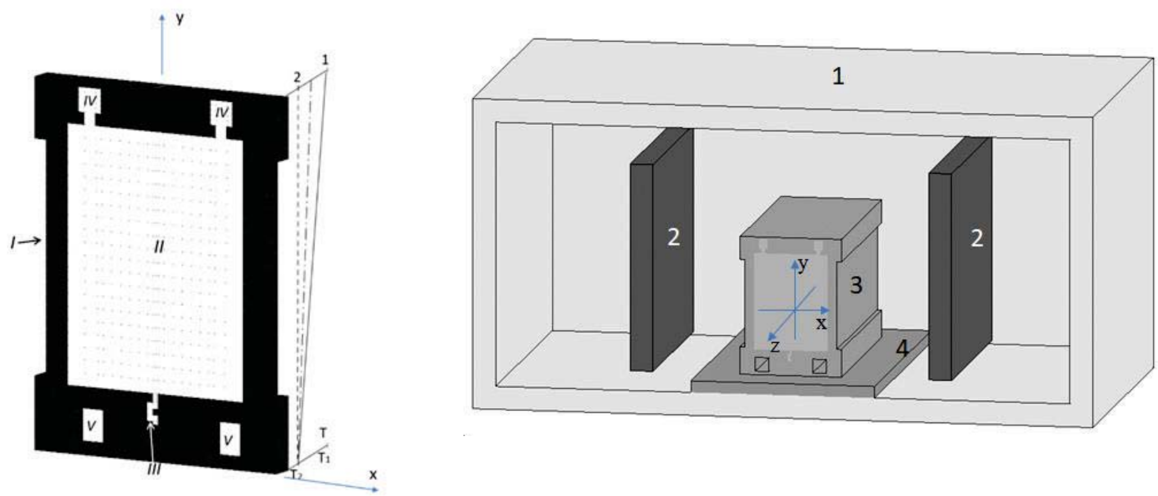

(a) (b)

FIGURE 1. Schemes of mathematical models:
(a) – cassette (shell – *I*, crystallizing material – *II*, seed crystal – *III*, holes for pouring melt – *IV* and holes for mounting cassettes – *V*);
(b) – hot zone (water-cooled chamber – 1, heater – 2, cassette block – 3, massive plate – 4)

The initial melt fills the cassette between two narrow graphite plates, along which a temperature gradient is supported. The advantage of this method is in possibility of simultaneous using a large number of gap layers between graphite plates. By means of it, a large number of TE wafers may be produced in one crystallization process. The polycrystal wafers obtained by this means have a higher mechanically hardness and its electrophysical properties are closely to single crystals.

During the process, it is possible to control the crystallization rate by operating the vertical temperature gradient, which affects on the crystallization front (FC) shape, too. It was experimentally established that the flat shape of FC provides a most effective texture of bismuth telluride wafers. However, a large curvature of FC shape causes the significant orientation deviations of the grains in produced polycrystal.

This paper presents an elaboration of theoretical-methodological approach for an analysis of heat and mass transfer processes during the cassette crystallization. This approach was implemented as three mathematical models: radiative-conductive heat transfer for whole design of hot zone, convective-conductive heat transfer for single growth cassette, and convective mass transfer for two-component melt of bismuth and tellurium in single growth cassette. The software realization of these mathematical models was performed on the basis of the finite difference and finite elements methods implemented in *CrystmoNet* software package [6].

HEAT TRANSFER IN HOT ZONE

The three-dimensional model for hot zone was developed with using finite element method. It contains the following components shown in Fig. 1b: a water-cooled steel chamber (1), heater (2), cassette block is (3), massive steel plate (4). The hot zone geometry is really complicated.

There are areas of hot zone components arrangement, which are not “connected.” For example, a heater is a geometrically isolated design, which carries out the heating of other hot zone components by thermal radiation.

The hot zone is equipped by a number of materials that differ by their thermophysical properties (see Table 1), which were taken from [7,8,9]. The temperatures of solidus T_s = 863K and liquidus T_l = 865K were fixed according to the state diagram of $Bi_2Te_3 - Sb_2Te_3$ system [10].

TABLE 1. Thermal physical parameters of hot zone components, including: melt (*l*) and crystalline (*s*) phases of bismuth telluride [6,7,8].

Material (Figure 1a, b)	**Density ρ [kg/m^3]**	**Thermal Conductivity λ [W/m×K]**	**Heat Capacity C_p [J/kg×K]**	**Emission ε**
Steel – *1, 4*	8000	15.0	500	0.15
Graphite – *2, 3*	2000	73.4	1500	0.8
Crystal – *s*	7690	2.9	173	not used
Melt – *l*	7850	6.3	179	not used

Heater (3) radiates a thermal flux to the cassette block (2). The heat conductively flows down onto the massive steel plate lying under cassette block. This design is located in closed chamber (1), its outer shell of which is maintained at room temperature due to the permanent water circulation.

The total sizes of hot zone components (*x*×*y*×*z*): chamber (27×13.5×14) cm^3, heater (1×9×9) cm^3, cassette block (4.4×6×10) cm^3, steel plate (8×0.5×14) cm^3.

In this case, mathematical modelling includes a numerical solution of heat transfer equation in complicated geometric region of hot zone with taking into account of its components having different thermophysical properties and taking into account of heat radiation and crystallization jointly.

The calculation results made it possible to identify the features of thermal processes, in particular, to establish the role of design factors (relative position and sizes of hot zone components.

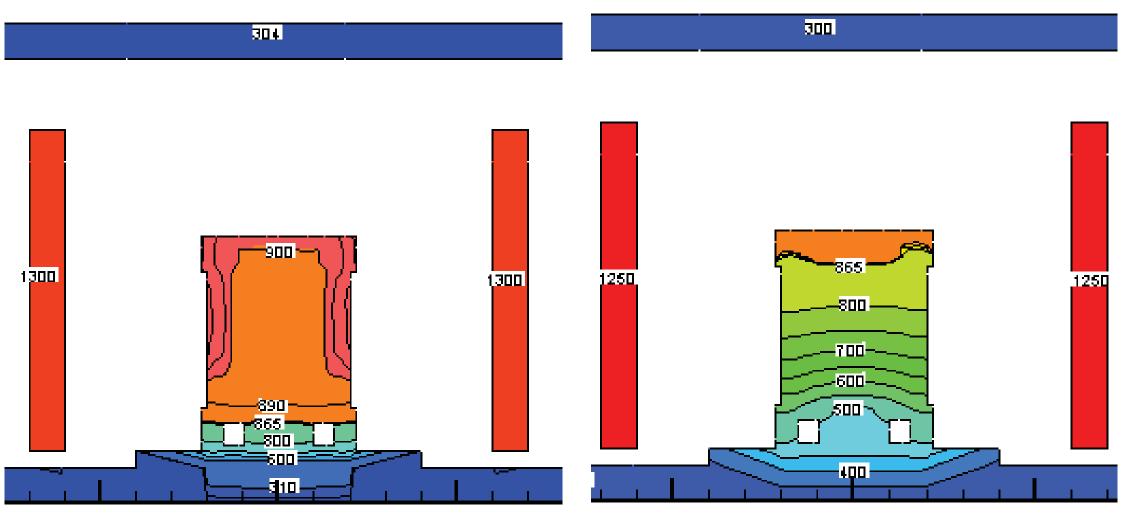

(a) (b)

FIGURE 2. Isotherms in hot zone and cassette block at heater power: a – 9kW and b – 7kW.
The FC shape corresponds to isotherm 865K

Let us consider the features of thermal field at the beginning and end of crystal growing processes.

According to the scheme shown in Figure 1a, at initial moment, a melt completely fills cavities *II*, *III* and *IV* under conditions of maintaining the fixed vertical temperature gradient (between minimum and maximum temperatures on the cassette bottom and top, correspondently). The cassette block is cooled by decreasing the heater power during crystal growth process.

The cassette block is located by such manner (Figure 1b) that a thermal radiation from the heater is directed to its lateral surface ($y \times z$). The surfaces ($x \times y$) face to a water-cooled chamber wall. Therefore, a cassettes block center is less warmed up. That may be seen from significantly curving upward isotherms in the center. Also, it may be noted, that this arrangement of cassette block creates not quite identical thermal conditions for cassettes located in center and at periphery of cassette block. In practice, this is confirmed by the different quality of grown central and peripheral wafers [11].

The process begins by pouring a melt into an internal cassette volume at temperature 900K. The initial heater temperature reaches 1300K, that corresponds to the heater power Q_H = 9kW. The distributions of isotherms in hot zone and cassette block are shown in Figure 2a. The analysis shows, that a central cassette part is heated more substantially in comparison with the lateral and bottom surfaces. The contact area of cassette bottom and massive steel plate lying on water-cooled chamber bottom supports the crystallization temperature (865K) and almost flat FC. Such cassette cooling does not allow to melt the crystalline seed (III) (see Figure 1a).

At final process stages, the heater temperature decreases to 1250K, that corresponds to decreasing the heater power to Q_H = 7kW. The isotherm 865K corresponding to FC shape has W-typed shape with a small sagging into crystal (Figure 2b).

HYDRODYNAMICS AND HEAT TRANSFER IN SINGLE CASSETTE

The crystallization process for separate cassette (Figure 1b) is considered similarly to above description for hot zone. It is assumed, that there is an intermediate crystallization area between crystal (solid fraction) and melt (liquid fraction). This crystallization area locates at temperatures T, which are higher the solidus temperature T_s = 863K and lower the liquidus temperature T_l = 865K. In heat transfer equation, the latent crystallization energy is taken into account as $Q = \rho_s L(\partial\varphi/\partial t)$, where the volume solid fraction in the two-phase area is set by following relation: $\varphi = (T - T_s)/(T_l - T_s)$.

The heat transfer equation for a melt is written as:

$$\rho_l C_l^p \left[\frac{\partial T}{\partial t} + (\boldsymbol{V}\nabla)T\right] = \lambda_l \Delta T \tag{1}$$

The Navier-Stokes and continuity equations are solved for determination of velocity vector $\boldsymbol{V}$ and pressure p in bismuth melt (Bi), taking into account of gravitational thermal convection using Boussinesq's approach:

$$\frac{\partial \boldsymbol{V}}{\partial t} + (\boldsymbol{V}\nabla)\boldsymbol{V} = -\frac{1}{\rho_l}\nabla p + \frac{\mu}{\rho_l}\Delta \boldsymbol{V} + \boldsymbol{g}\beta_T T \tag{2}$$

$$div\boldsymbol{V} = 0 \tag{3}$$

where $\boldsymbol{g}$ is gravity vector, β_T is thermal expansion coefficient, μ is coefficient of melt dynamic viscosity.

Eqs. (2),(3) are solved jointly with transfer equation for tellurium (Te) concentration:

$$\frac{\partial M}{\partial t} + (\boldsymbol{V}\nabla)M = D\Delta M \tag{4}$$

where $M = \rho_l C$ is Te concentration in melt [kg/m^3], C is relative mass of Te per 1kg of melt.

The following boundary conditions are set into the calculations for velocity and concentration distributions:

– the upper cassette boundary is stationary at Te concentration $C = C_{eo}$;

– the lateral cassette surfaces are stationary at a zero flux of Te concentration;

– the FC shape is stationary with taking into account of following mass balance relation:

$$\rho_l D \frac{\partial C}{\partial n} = R(\rho_s - C_e \rho_l) \tag{5}$$

where R is FC rate in normal direction $\boldsymbol{n}$. The input parameters for heat and Te mass transfer calculations in crystal and melt are given in Table 2.

TABLE 2. The input parameters of heat and Te mass transfer.

Parameter	Symbol	Dimension	Value
Melt Dynamic Viscosity	μ	kg/m×s	1.2×10^{-3}
Crystal Heat Capacity	C_s^p	J/kg×K	127
Melt Heat Capacity	C_l^p	J/kg×K	141
Melt Thermal Conductivity	λ_l	W/m×K	13
Crystal Thermal Conductivity	λ_s	W/m×K	2.9
Melt Thermal Expansion	β_T	K^{-1}	2.8×10^{-4}
Melt Te Diffusion Coefficient	D	m^2/s	5.4×10^{-10}
Melt Density	ρ_l	kg/m^3	10270
Crystal Density	ρ_s	kg/m^3	7690
Equilibrium Te Concentration on FC	C_e	dimensionless	0.5
Initial Melt Te Concentration	C_{eo}	dimensionless	0.7

The problem of crystallization rate increasing is very relevant because of this increases a crystal growth productivity by this cassette Bridgman method. However, the experimental attempts for significantly acceleration of crystallization process are accompanied by heat balance violation in growth cassette. This leads to the significant FC curvature and dendritic growth. The ideal case corresponds to the cassette cooling at stable vertical temperature gradient, which should be supported and gradual decreased during whole process time. This provides an absence of intense melt convection and supports a flat FC shape.

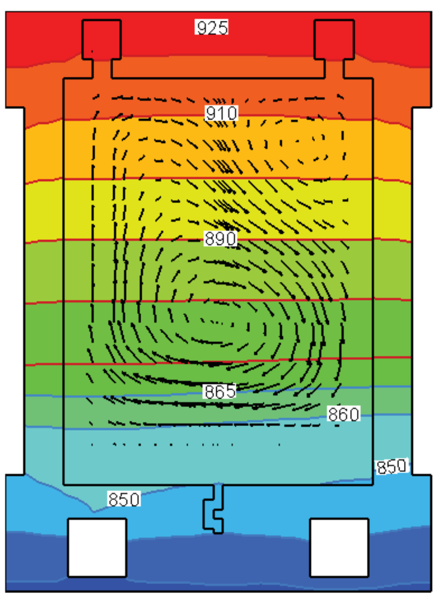

FIGURE 3. Vortex structures and isotherms [K] at the beginning of crystallization under conditions of unstable temperature stratification, which causes convection during inhomogeneous cooling of the cassette bottom.

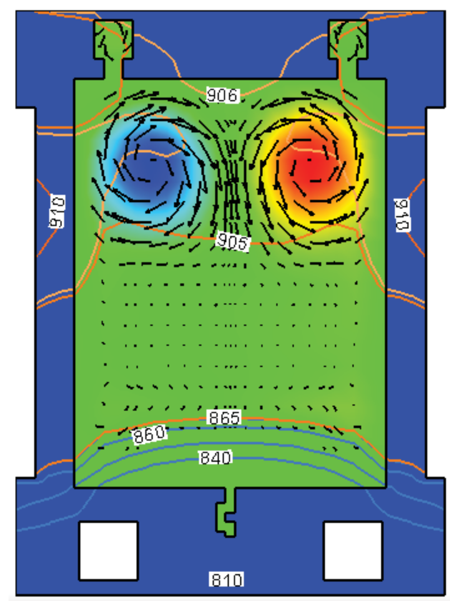

FIGURE 4. Vortex structures and isotherms [K] under conditions of unstable vertical temperature stratification, which causes symmetric and weak convective melt motion during slow cassette cooling at $V = 0.15$mm/min.

The convective model was implemented for two-dimensional case. The boundary conditions were set using calculation results of three-dimensional radiation-conductive model for the hot zone. The heating conditions of cassette block were applied for calculations of thermal fields in a separate cassette at beginning and final crystallization stages. Vertically stable temperature stratification provides only conductive heat transfer at beginning crystallization stage. May be noted, the FC has convex shape, which is smoothed during the process.

A stable vertical temperature gradient was maintained at all stages of the crystallization process (see profiles *1*–*3* in Figure 1a). Thus, a melt convection is practically suppressed and the distribution of isotherms corresponds to the conductive heat transfer in a melt under the conditions of a stable vertical temperature gradient and an absence of design and thermal asymmetry during whole growth process.

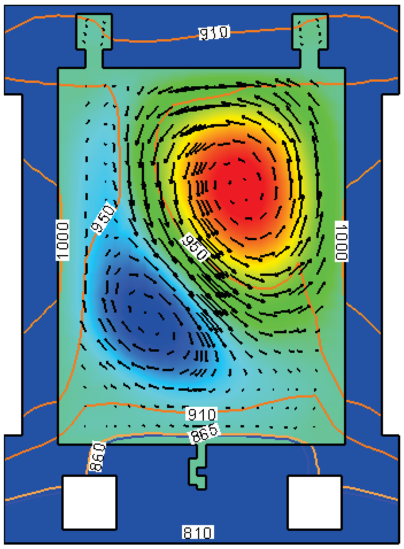

FIGURE 5. Vortex structures and isotherms [K] under conditions of unstable vertical temperature stratification during rapid cassette cooling at the rate $V = 1.2$mm/min.

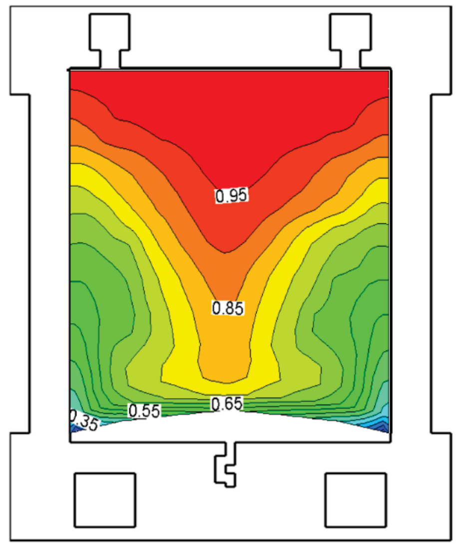

FIGURE 6. Te mass transfer in Bi melt: isolines of concentration C/C_{eo} in the cassette volume at a stable temperature stratification, but for a high crystallization rate $R_3 = 6$ mm/min.

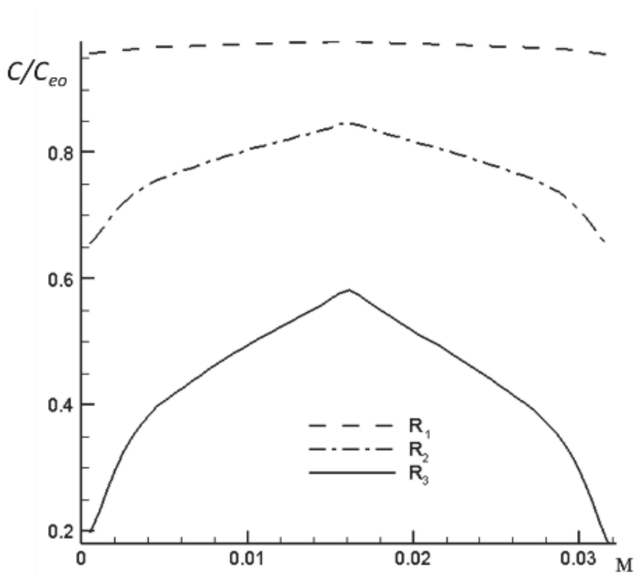

FIGURE 7. Te mass transfer in Bi melt: radial Te profiles C/C_{eo} long of FC shape at various crystallization rates (R_1 = 0.3, R_2 = 3, R_3 = 6mm/min).

However, this situation changes sharply in cassette at thermal asymmetry occurrence, which is caused by significantly inhomogeneous (for direction *x*, see Figure 1a) cooling of the massive plate. Mathematical modeling revealed the features of such thermal situation (Figure 3). In the case of such cooling, the vortices shape of becomes non unidentical. The most significant vortex flows around the FC shape at rather high velocity ~ 0.034cm/s. It leads to FC shape curvature (see the isotherm 865K in Figure 3).

Another reason causing convective melt motion in cassette is caused by its nonuniform vertically heating. The slow cassette cooling at FC velocity R = 0.15mm/min corresponds to the symmetric vortex structures occurrence and weak convective flow, which ensures the slightly FC convex shape (Figure 4).

However, the attempts of quick cassette cooling by a sharp decreasing heater power are carried out in technological experiments permanently. In practice, this records a significant FC shape curvature and the dendritic growth occurrence. The corresponding calculations show that this is caused by an appearance of unstable vertical temperature gradient, which leads to an asymmetric vortex motion.

The small design inhomogeneity of cassette causes the vortices and isotherms asymmetry (Figure 5) at rapid cooling (R = 1.2mm/min). The vortex asymmetry is caused by small lateral design differences of the cassette. The arising intense convection significantly changes a thermal field both in melt volume and near the FC shape.

The effect of melt convection creates a substantial inhomogeneous volume Te concentration distribution at R = 6 mm/min and its flux into the crystal becomes much larger (Figure 6). The significant decrease of Te concentration is observed for temperature T = 865K, that violates equilibrium composition for Bi_2Te_3 compound crystallization according to the state diagram [10].

For comparison, the radial Te concentration distributions along of FC shape are shown in Figure 7. Their analysis shows, that a radial homogeneity of Te concentration distribution is observed only at low crystallization rates R = 0.3 mm/min. On the contrary, the radial changes of Te concentration become significant for large R values. Thus, a radial inhomogeneity arises in the Te distribution as a result of convection. A violation of melt composition near FC shape may be as a reason of instability of bismuth telluride crystalline phase formation.

CONCLUSION

The mathematical models of crystallization in cassettes have been elaborated as the Bridgman method modification. The elaborated model of conductive-radiative heat transfer for whole hot zone has became as basis of parametric calculations, on which an affect of different design components, including their locations and temperatures, has been analyzed and the thermal conditions at cassette block boundaries were established.

The calculations for growth cassette using the conductive-convective model showed, that the construct and boundary thermal conditions asymmetry, as well as the unstable vertical temperature gradient, result to the convective vortices and significant FC shape non-flatness.

The calculations using convective Te mass transfer showed that a large crystallization rate significantly increases Te flux into crystal. Because of it, a melt composition near FC shape is changed, that becomes a potential reason of dendritic growth onset. The reliability of these calculation results was verified on a number of tests, in which an influence of cooling rates on FC shape was analyzed at cassette cooling rates corresponding to the growth processes of bismuth telluride polycrystals.

ACKNOWLEDGMENTS

This work was performed on the computational base of IPMech RAS (work No. AAAA-A20-120011690136-2) with the support of the Russian Foundation for Basic Research (grant No. 18-02-00036).

REFERANCES

1. J.-T. Im, *Grain Refinement and Texture Development of Cast BiSb Alloy via Severe Plastic Deformation* (Yeung University, S. Korea, 2007), 113p.
2. D.I. Bogomolov, V.T. Bublik, N.A. Verezub, A.I. Prostomolotov, and N.Yu. Tabachkova (2018) *Russian Electronics* **47**(8), 544–552.
3. V.F. Ponomarev and D.G. Ryabinin, U.S. Patent No. 0,282,284 (11 November 2010).
4. Ju.M. Belov, M.P. Volkov, and S.M. Manjakin, RU Patent No. 2,181,516 (20 April 2002).
5. V.D. Demcheglo, A.I. Voronin, N.Yu. Tabachkova, V.T. Bublik, and V.F. Ponomaryov (2017) *Semiconductors/Physics of the Solid State* **51**(8), 1064–1067.

6. A. Prostomolotov, H. Ilyasov, and N. Verezub (2013) *Science and Technology* **3(2A)**, 18–25.
7. Ja.B. Magomedov, G.G. Gadzhiev, and Z.M. Omarov (2013) *Phase Transitions, Interfaces and Nanotechnology* **9**, 1–5.
8. V.M. Glazov, S.N. Chizhevskaya, and N.N. Glagoleva, *Liquid Semiconductors* (Nauka, Moscow, 1968), 246p.
9. A.S. Pashinkin and M.S. Mikhailova (2015) *Proceedings of Universities Electronics* **20**(2), 198–200.
10. T. Caillat *et al* (1992) *J. of Physics and Chemistry of Solids* **53**(2), 227–232.
11. A.I. Voronin, A.P. Novitskii, Y.Z. Ashim, T.M. Inerbaev, N.Y. Tabachkova, V.T. Bublik, and V.V. Khovaylo (2019) *J. of Electronic Materials* **48**(4), 1932–1938.